GDP Release from the Open Conformation of Gα Requires Allosteric Signaling from the Agonist Bound Human β_2 Adrenergic Receptor

Vikash Kumar[1#], Hannah Hoag[2#], Safaa Sader[2], Nicolas Scorese[2], Haiguang Liu[1*] and Chun Wu[2*]

[1] Complex Systems Division, Beijing Computational Science Research Center, Haidian district, Beijing, 100193 China

[2] College of Science and Mathematics, Rowan University, Glassboro, NJ 08028 USA

[#] Both authors have contributed equally

*To whom correspondence should be addressed: wuc@rowan.edu or hgliu@csrc.ac.cn

Abstract

G-protein-coupled receptors (GPCRs) transmit signals into the cell in response to ligand binding at its extracellular domain, which is characterized by coupling of agonist induced receptor conformational change to guanine nucleotide (GDP) exchange with GTP on a heterotrimeric (αβγ) guanine nucleotide-binding protein (G-protein), leading to the activation of the G-protein. The signal transduction mechanisms have been widely researched *in vivo* and *in silico*. However, coordinated communication from stimulating ligands to the bound GDP still remains elusive. In the present study, we used microsecond (μS) molecular dynamic (MD) simulations to directly probe the communication from beta2 adrenergic receptor (β_2AR) with an agonist or an antagonist or no ligand to GDP bound to the open conformation of Gα protein. MM-GBSA calculation results indicated either agonist or antagonist destabilized the binding between the receptor and the G-protein, but agonist cause a higher level destabilization than antagonist. This is consistent with the role of agonist in the activation of G-protein. Interestingly, while GDP remained bound with the Gα-protein for the two inactive systems (antagonist bound and apo form), GDP dissociated from the open conformation of Gα protein for the agonist activated system. Data obtained from MD simulations indicated that the receptor and the Gα subunit play a big role in coordinated communication and nucleotide exchange. Based on residue interaction network analysis, we observed that engagement of agonist bound β_2AR with α5 helix of G_α is essential for the GDP release and the residues in phosphate-binding loop (P-loop), α1 helix, and α5 helix play very important roles in the GDP release. The insights on GPCR/G-protein communication will facilitate the rational design of agonists and antagonists that target both active and inactive GPCR binding pockets, leading to more precise drugs.

Introduction

Guanine nucleotide-binding proteins, known as G-proteins, are a family of proteins that act as molecular switches inside the cell. Receptors on the cell surface coupled to heterotrimeric G-proteins are known as G-protein coupled receptors (GPCRs). The GPCR protein family is one of the largest membrane protein families and is encoded by over 800 genes in the human genome [1]. Targeting the GPCR family can produce therapeutic agents that reduce neurological disorders, asthma, chronic obstructive pulmonary disease, cancer, and inflammatory diseases [2]. GPCR signal transduction mechanisms have been widely researched, including pathways and response [3]. Although ligand-GPCR interactions and GPCR-trimeric protein interactions have been extensively studied [2], coordinated communication from stimulating ligands to their effector GDP still remains elusive. GPCR conformational changes and subsequent nucleotide exchange is not well understood. Understanding GPCR conformational changes and G-protein stimulation can be very beneficial in developing novel drugs for various diseases.

The heterotrimeric (αβγ) G-protein, in its inactive form, is bound to guanosine diphosphate (GDP). Upon activation of the GPCR by an agonist, the G-protein undergoes a significant conformational change, leading to that the GDP is released and guanosine triphosphate (GTP) spontaneously binds to the vacated binding site. When GDP is released and the G-protein is bound to GTP, the G-protein dissociates into a Gα subunit and a Gβγ complex. The Gα subunit is evolutionarily related to the Ras family of proteins. Based on sequences and functions, Gα proteins have been divided into four main families (**Figure S1**), Gαs, Gαq/11, $G\alpha_i/G\alpha_o$ and $G\alpha_{12}/G\alpha_{13}$ [4]. All Gα subunit contains two domains (**Figure S2**), the Ras domain (GαRas) and the

alpha-helical domain (GαAH) [4]. The GαRas domain contains the nucleotide binding site and the GαAH domain is responsible for domain separation by moving away from GαRas [5].

The β_2AR (**Figure 1**) is often used as a model system to study the GPCR family. Chung et al., used the β_2 adrenergic receptor-G protein complex to examine nucleotide exchange [6]. They speculated that the release of GDP is initialized by the interactions between intracellular loop 2 (ICL2) of β_2AR and αN helix of GαS and coupled to the subsequent structural changes in the highly conserved peptide-binding loop (P-loop). Dror et al., addressed important questions about domain separation and GDP release using β_2AR [7]. They carried out atomic-level MD simulations of heterotrimeric G-proteins with and without bound GPCR. Using the crystal structure of the β_2AR- G-protein complex (nucleotide-free), 66 simulations were performed using lengths of up to 50 μs each [7]. They also completed simulations of a GDP-bound G-protein without β_2AR. In these simulations, the GαRas and GαAH domains separated from one another. This open conformation of the Gα subunit resembles the nucleotide-free β_2AR-G protein complex conformation. Although domain separation occurred, GDP remained bound throughout the simulations. Even removal of the GαAH did not promote GDP leaving GαRas domain in simulation. Separation occurs spontaneously even when GPCR is not bound to the heterotrimeric G protein. Above findings by Dror et al., suggest that domain separation is necessary but not sufficient for GDP release. Furthermore, a weakening of nucleotide-Ras domain contacts is also required. The shift up of α5 helix, induced by an activated β_2AR, favors GDP detachment and nucleotide exchange through conformational changes at the GαRas domain [7]. Computational studies of thromboxane A2 receptor (TXA_2R)-Gq complex revealed that contacts between C-terminus of α5 and receptor are major players in the receptor catalyzed motion of the αH domain and eventually the release of GDP [8]. Recent computational study suggests that the rate limiting

step for GDP release involves translation or tilting of α5 helix [9]. We refer these models as a "α5-centered" model for the GDP release. Despite these progresses, there is little information on how binding of Gα to an activated β_2AR weakens the interaction between GDP and Ras domain, promoting GDP release. For example, because α4 and αN are also in contact with IntraCellular Loop 2 and 3 (ICL2 and ICL3) of the receptor, respectively, do they also play some roles in the conformational change at the GαRas domain that weakens the GDP affinity? What are the major communication pathways from the agonist to GDP? What are the critical residues in these pathways? Can those key residues explain the mutagenesis experimental data? What is the receptor and G-protein response when the agonist is changed to an antagonist or no ligand? In present study, we have investigated the communication between agonist or antagonist bound β_2AR and GDP bound Gα protein. The simulation results highlighted the important regions in Gα which are responsible for GDP release. Findings from the present study provide insight on GPCR-G-protein activation and GDP release mechnism.

Materials and Methods

Homology modeling of human β2-adrenergic-Gαβγ complex

Rasmussen et al. has determined a crystal structure of the chimeric β2-Adrenergic receptor in complex with a G_s-protein complex [5]. In the crystal structure (PDB ID 3SN6), human β2-adrenergic receptor (30-341) has two missing regions (176-178 and 240-264) which belong to a part of extracellular loop2 (ECL2) and intracellular loop3 (ICL3) respectively. Crystal structure has Gα and Gγ from *Bos taurus* (domestic cattle) and G_β from *Rattus norvegicus* (brown rat). Using the pre-aligned crystal structure in membrane from the OPM web server[10] as a template, we applied homology modeling procedure to complete the short missing region of β_2AR (172-

178) and to construct a full model of human β_2AR-G$\alpha\beta\gamma$ complex. The template also contains agonist BI-167107, which was incorporated into the modeled complex. To get the binding pose of an antagonist (alprenolol), we superimposed the homology model of β_2AR with another crystal structure of β_2AR in complex with alprenolol (PDB: 3NYA) [11], and thus the crystal pose of alprenolol was adopted.

Molecular docking of GDP

Protein structures were prepared using Maestro protein preparation wizard **(**Schrödinger Release 2019-4**:** Maestro, Schrödinger, LLC, New York, NY, 2019). First, the charge state of preprocessed complexes was optimized at pH=7. Second, a restrained minimization was performed to relax the protein structures using OPLS3 force field. The prepared complexes were used to generate docking grid files. Site identified by the site detection tool was specified as the binding site for the GDP. The prepared GDP was docked into the grid using Glide XP scoring function with default procedures and parameters **(**Schrödinger Release 2019-4**:** Glide, Schrödinger, LLC, New York, NY, 2019). The receptor grid was generated using Van der Waals scaling factor of 1 and partial charge cutoff 0.25. The ligand docking was performed using a ligand-centered grid using OPLS3 force field. The obtained complex from the Glide XP docking was further subjected to an induced fit docking (IFD) to obtain the final complex. To confirm the GDP binding site in our homology model we superimposed the closed Gα subunit containing GDP (PDB: 1GOT) [12] with our human Gα subunit containing the docked GDP.

System setup for all-atom Molecular Dynamics Simulations

Each of the three pre-aligned complexes (the agonist, antagonist and apo complex systems) was placed in a membrane consisting of phosphatidylcholines (POPC). Then, each system was

solvated in an orthorhombic water box with a 10 Å water buffer and neutralized by Na^+ ions. Additional Na^+ and Cl^- ions were added to reach 0.15 M NaCl salt concentration. The total number of atoms for each system was roughly ~139,000 and the system size with membrane in x, y, z directions was ~100.1 Å, ~102.2 Å and ~133.4 Å, respectively. POPC is the most common lipid in animal cells [13], and POPC lipid bilayer is prototypical model and wildly used in MD simulations of membrane proteins [14, 15], some of which were along with OPLS-AA (optimized potential for liquid simulations-all atom) force field [16, 17]. Simple point-charge (SPC) [18] water model was used, and OPLS3 force field [19] was used to model protein, lipids, ligand and ions.

Using Desmond module (Schrödinger Release 2019-4: Desmond Molecular Dynamics System, D. E. Shaw Research, New York, NY, 2019.), the system was first relaxed using the default relaxation protocol for membrane proteins. This relaxation protocol consists of eight stages: 1). Minimization with restraints on solute heavy atoms; 2) Minimization without any restraints; 3). Simulation with heating from 0 K to 300 K, H_2O barrier and gradual restraining; 4). Simulation under the NPT ensemble (constant number of particles, constant pressure of 1 bar and constant temperature of 300 K) with H_2O barrier and with heavy atoms restrained; 5) Simulation under the NPT ensemble with equilibration of solvent and lipids; 6). Simulation under the NPT ensemble with protein heavy atoms annealing from 10.0 kcal/mol to 2.0 kcal/mol; 7). Simulation under the NPT ensemble with Cα atoms restrained at 2 kcal/mol; and 8) Simulation for 1.5 ns under the NPT ensemble with no restraints. After the relaxation, each system was subject to a 3000.0 ns simulation for the NPT ensemble using the default protocol. As a control, a second set of simulation trajectories (each is 1000.0 ns) were generated. Temperature was controlled using the Nosé-Hoover chain coupling scheme with a coupling constant of 1.0 ps. Pressure was

controlled using the Martyna-Tuckerman-Klein chain coupling scheme with a coupling constant of 2.0 ps. M-SHAKE was applied to constrain all bonds connecting hydrogen atoms, enabling a 2.0 fs time step in the simulations. The k-space Gaussian split Ewald method was used to treat long-range electrostatic interactions under periodic boundary conditions (charge grid spacing of ~1.0 Å, and direct sum tolerance of 10^{-9}). The cutoff distance for short-range non-bonded interactions was 9 Å, with the long-range van der Waals interactions based on a uniform density approximation. To reduce the computation, non-bonded forces were calculated using an r-RESPA integrator where the short-range forces were updated every step and the long range forces were updated every three steps. The trajectories were saved at 40.0 ps intervals for analysis. The SCHRODINGER's Simulation Interactions Diagram (SID) tool and VMD [20] were used to analyze the simulation data.

Residues interaction network analysis

For creation of network map, Cα atoms were considered as nodes. Edges were drawn if nodes were within cutoff distance of 4.5 Å for at least 75% of the trajectory. The early study has shown that the effect of the cutoff parameter on the network properties is minor when the cutoff distance ~ 4.5Å [21]. CARMA tool [22] was used to calculate cross correlation map of Cα atoms of complexes over 1.2 µs trajectory. The edge distances d_{ij} are derived from the pairwise correlations (C_{ij}) between Cα atoms [21] **.** Where d_{ij} defines the probability of information transfer across a given edge.

$$d_{ij} = -\log(|C_{ij}|)$$

$$C_{ij} = \frac{\langle \Delta\vec{r}_i(t) \cdot \Delta\vec{r}_j(t) \rangle}{\left(\Delta\vec{r}_i(t)^2 \cdot \Delta\vec{r}_j(t)^2\right)^{1/2}}$$

Where $\Delta\vec{r}_i(t) = \vec{r}_i(t) - \langle\vec{r}_i(t)\rangle$ and $\vec{r}_i(t)$ is the position of the atom corresponding to i^{th} node [21]. C_{ij} is the probability of transfer information across a given edge. Networks were visualized using the "NetworkView" module [23] of the VMD. After selection of start and sink nodes, "subopt" program was used to calculate optimal and suboptimal paths between them. In addition to weighting networks based on the correlated motion in the simulation trajectory, the networks may also be weighted based on the strength on interactions within a single structure as demonstrated by Vishveshwara and cowworkers[24] [25]. Dynamic network models have been effectively used to decipher allosteric and communication pathways in transmembrane proteins[26]. Using a dynamic network model, Schneider et al. have successfully identified different pathways leading to biased and unbiased activation of the μ-Opioid Receptor[27]. Jiang et al. have also successfully used a network model to elucidate the dynamic and allosteric properties of three GPCR homodimers [28].

Binding energy calculations

Molecular Mechanism-General Born Surface Area (MM-GBSA)[29] binding energies were calculated on the frames in the last 200 ns of the combined trajectories for each system. OPLS3 force field, VSGB 2.0 solvation model [30] and the default Prime procedure was used for the MM-GBSA calculation. The default procedure consists of three steps: Receptor alone (minimization), Ligand alone (minimization), Receptor-ligand complex (minimization). The total binding free energy equation is: $\Delta G_{(bind)} = E_{complex\ (minimized)} - (E_{ligand(minimized)} + E_{receptor(minimized)})$. There are three components analyzed: $E_{electrostatics}$ ($H_{bond} + E_{coulomb} + E_{GB\_solvation}$), E_{vdW} ($E_{vdW} + E_{\pi\text{-}\pi\ stacking} + E_{self\text{-}contact}$), and $E_{lipophilic}$.

Results and discussions

Agonist and antagonist bound human β2AR-Gα-protein complexes

We used crystal structure of chimeric human β2AR-Gprotein complex (PDB ID 3SN6) containing agonist BI-167107 as the template for homology modeling. Sequence alignment showed that different types of Gα share significant homology with each other (**Figure S1**). The chimeric human crystal structure is shown in **Figure S2**. To confirm the GDP binding site in the homology model, we aligned the closed Gα subunit containing GDP (PDB: 1GOT**)** with human Gα subunit containing the docked GDP (**Figure S3 and S4**). Compared to the co-crystallized conformation in the closed form of Gα, the Gα with docked GDP has a similar conformation to that in the open form. Structural alignment of closed and open forms of Gα showed that the RAS domain does not undergo large conformational change during GDP release. Secondary structure elements of RAS domain are shown in **Figure S5**. 3D coordinates of antagonist (alprenolol) was transferred to the homology model after superposing the modelled human β2AR with another crystal structure containing alprenolol (PDB: 3NYA**)**. Binding pocket residues interacting with BI-167107, alprenolol and GDP are shown in **Figure 1**. The full complexes in three states (agonist bound, antagonist bound, and apo) are summarized in **Figure 2**.

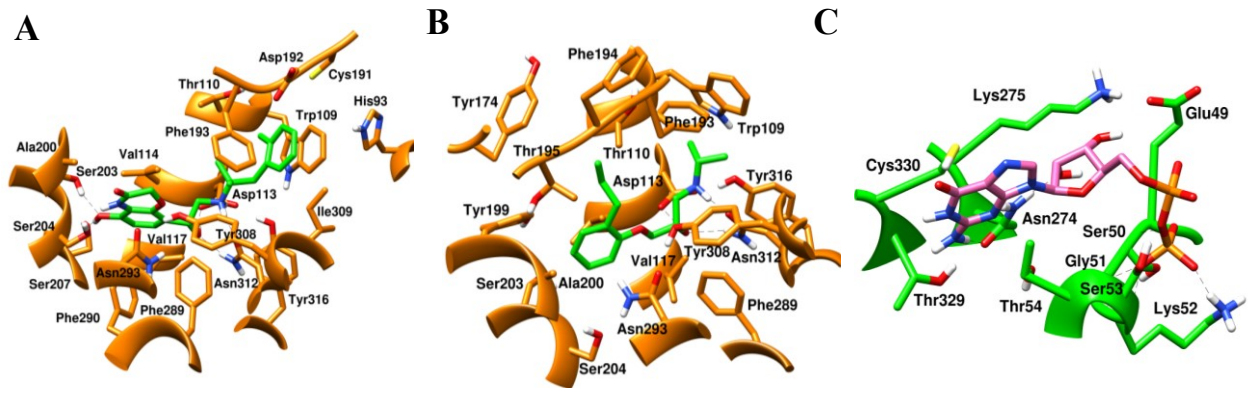

Figure 1. Initial conformations of (A) agonist (green), (B) antagonist (green) and (C) GDP (pink) in their corresponding binding pocket in β_2AR (for agonist and antagonist) and Gαq (for GDP).

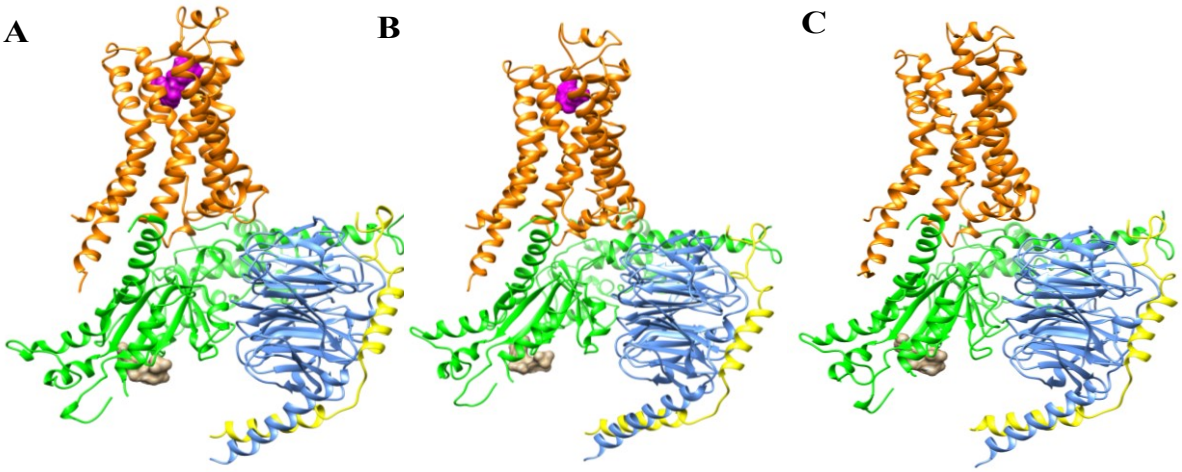

Figure 2. β_2AR-G-protein complexes with GDP (tan colour and surface representation) and (A) Agonist (magenta colour and surface representation) (B) Antagonist (magenta colour and surface representation) and (C) without agonist or antagonist (apo system). Cartoon representation of β_2AR, Gαq, Gβ and Gγ are shown in orange, green, blue and yellow colours respectively. In **S1** and **S2 Tables**, residues of β_2AR and Gαq are listed according to the GPCR naming scheme and common Gα naming scheme, respectively.

Effect of agonist and antagonist on human β_2AR-Gαq complex

Backbone root mean square deviation (RMSD) analyses showed that all systems have reached to the steady state with the progress of MD simulation. The RMSD of different components of the β_2AR-G-protein complexes are shown in **Figure S6 and S7**. In the agonist bound system (**Figure S6A and S7A**), there is a clear gap in RMSD values between the components containing the Gα subunit and the components that do not, thus forming two groups. The full complex, the G-protein and the Gα subunit all have RMSD values of about 5 Å or higher, while the individual subunits (β_2AR, Gβ, Gγ) and the Gβ-γ complex have RMSD values between 2-4 Å. The same separation is seen in the antagonist complex (**Figure S6B** and **S7B).** The 3μs trajectory of apo complex (**Figure S6C**) does not have a visible separation between groups, and the Gγ subunit is comparative in RMSD values to the Gα subunit. However, the second trajectory of apo complex (**Figure S7C**) depicted a small separation between groups. In agonist bound system, larger separation denotes destabilization of the β_2AR-G$\alpha\beta\gamma$ interface.

Cα-RMSF analysis (**Figure S8 and S9**) of β_2AR showed that at ECL2 there is slightly more fluctuation in the agonist bound β_2AR. At ICL3, the fluctuation in the agonist bound β_2AR is nearly doubled compared to the case of antagonist bound β_2AR. ICL3 is the largest ICL and the loop in closest contact with the G-protein. Residues in the ICL3 make contacts with α5 helix of Gα [31]. The α5 helix is the last helix of the Ras domain and it is in direct contact with the β_2AR. In **Figure S8B,** there are visibly larger fluctuations in the antagonist complex, as compared to the agonist complex in the alpha helical domain of the Gα subunit. In second trajectory (**Figure S9B**), alpha helical domain in the agonist bound system showed larger fluctuations compared to antagonist bound and apo systems. However, in the first trajectory, Ras domain for the agonist Gα subunit there is more fluctuation at α4, α5 and β6. In **Figure S8C,** there is a similar level of

fluctuations in the Gβ subunit for the agonist as compared to the antagonist. In **Figure S8D**, compared to agonist and antagonist complexes, there is larger fluctuation in the Gγ subunit for the apo complex, but similar fluctuation in the second helix for both subunits. In second trajectories (**Figure S9C and S9D)**, we observed that Gβ and Gγ subunits of agonist complex showed higher fluctuation than antagonist bound and apo complexes. After comparison of RMSF profiles of both trajectories for the three systems we see that while the β_2AR and the Gβ subunit have smaller fluctuation (1.95Å and 1.66Å respectively), the Gα subunit and the N-terminal part of the Gγ subunit have much larger fluctuation (2.33Å and 4.89Å respectively), suggesting the latter parts are the response regions where the larger conformation change can be induced.

The ligand-β_2AR contacts are summarized in **Table 1**. The contact histograms of agonist and antagonist are also shown in **Figure S10**. Asp $113^{3.32}$, Phe 193^{E2}, Phe $290^{6.52}$ and Asn $312^{7.39}$ are in contact with both the agonist and antagonist for at least 30.0% of the 3μs simulations. The agonist and antagonist interact with residues mainly from TM 3, 5, 6 and 7.

Table 1: Ligand-Receptor Contacts

Agonist	Antagonist
$W109^{3.28}$	$D113^{3.32}$
$D113^{3.32}$	$F193^{E2}$
$F193^{E2}$	$F290^{6.52}$
$S203^{5.42}$	$N312^{7.39}$
$S207^{5.46}$	$V114^{3.33}$*
$F290^{6.52}$	$F289^{6.51}$*
$N293^{6.55}$	$Y308^{7.35}$*
$N312^{7.39}$	$I309^{7.36}$*

*Not in contact more than 30.0% of simulation time

We analyzed the effects of agonist and antagonist on molecular switches of β_2AR. Ionic lock between $Asp130^{3.49}$ and $Arg131^{3.50}$ was found to be broken in both systems. Even in the absence of agonist or antagonist, ionic lock was broken. On the other hand, the transmission switch was intact in all three systems. Only tyrosine toggle switch was affected by the binding of agonist uniquely. We observed toggle of side chain of tyrosine in the agonist bound β_2AR. The torsion angle analysis was carried out for the chi1 and chi2 angles within $Y326^{7.53}$ of the tyrosine toggle switch (**Figure S11 and S12**). The chi1 analysis shows a relatively flat plot for the agonist bound and apo complexes (**Figure S11A and C**). The antagonist complex showed change **(Figure S11B)** early in the simulation trajectory (~100 ns), but then remained stable for the remainder of the trajectory. Chi2 analysis (**Figure S12**) shows much larger changes within all three systems. The agonist complex (**Figure S12A** and **D**) is the only system which showed similar rotameric toggle of $Y326^{7.53}$. In the first trajectory of antagonist system (**Figure S12B**), chi2 of $Y326^{7.53}$ took various values between -180 and 180 degrees. However, in second trajectory of antagonist system (**Figure S12E**), chi2 showed values between 60 to 120 degrees. In both first and second trajectories of apo system (Figure **S12C** and **F**), Y326 appeared to take various values between -

180 to 180 degrees. We observed that Y326$^{7.53}$ interacts with the Arg131$^{3.50}$ in all three complexes.

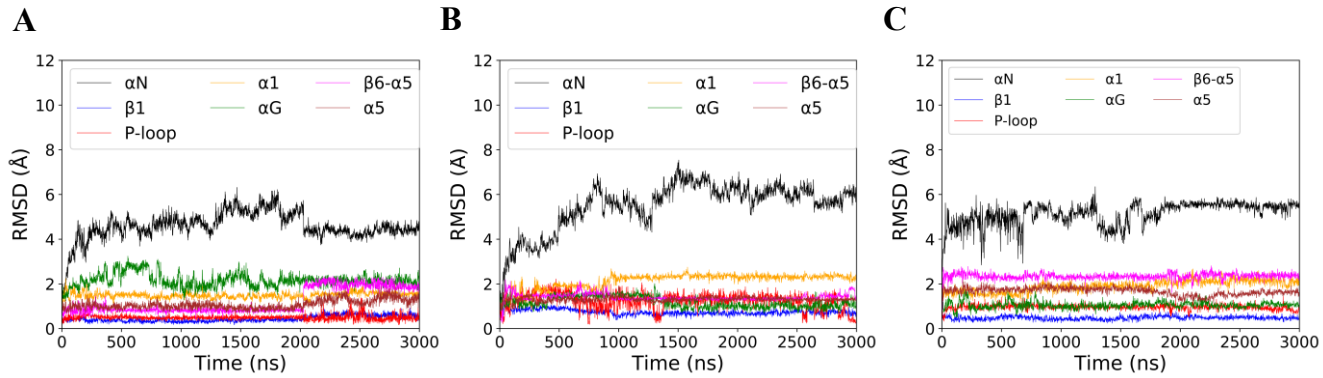

Figure 3: RMSD of different regions of $G_{\alpha q}$. Agonist bound system (A) antagonist bound system (B) and apo system (C).

We also investigated the effects of agonist and antagonist on different regions of Gαq subunit. RMSD analysis for the Gα-N-terminal, β1, P-loop, α1, αG, β6- α5 loop and α5 helix is shown in **Figure 3**. In agonist bound and apo systems (**Figure 3A and C**), RMSD values for the αN helix values were below 7Å. However, in antagonist bound system (**Figure 3B**), αN helix showed deviation greater than 7Å. In the agonist bound system (**Figure 3A**), αG showed higher RMSD than antagonist bound and apo system. We measured the distances between center-of-mass of the α5 helix and GDP, and between the center-of-mass of the β6-α5 loop and GDP (**Figure S13**). The apo complex remains constant for both the α5 helix and the β6-α5 loop with values of approximately 25 Å and 15 Å, respectively. The antagonist bound complex showed minor changes throughout the analysis for both measurements. The α5 helix distance starts around 30-31 Å and ends at approximately 27 Å. The decrease is gradual with little to no fluctuation during the simulation. The β6-α5 loop distance shows similar results for the antagonist bound system. The distance stays between 18-22 Å for the first 600 ns then decreases to about 13-15 Å for the

remainder of the simulation. The β6-α5 distance in agonist bound system begins at approximately 11 Å then quickly begins to fluctuate between 12-22 Å until the simulation reaches approximately 800 ns. At 800 ns the distance was about 26 Å then reduced to 9 Å. At 950 ns, the distance increased again to 23 Å before GDP begins to move out of the binding pocket. GDP appears to leave the binding pocket completely at about 1170 ns where the distance jumps to above 40 Å.

MM-GBSA binding energies indicate that the agonist destabilizes the GPCR-G-protein complex

MM-GBSA energy calculations were carried out at three interfaces of the β_2AR-G-protein complex, as described in the method section. These results summarized in **Table 2** indicate that the agonist binds more favorable to the β_2AR binding pocket than the antagonist by -60 kcal/mol. However, at the β_2AR-G-protein interface, the free energy binding is much more favorable for the antagonist system at -237 kcal/mol as compared to the agonist system at -163 kcal/mol. The apo complex was even more favorable at -249 kcal/mol for the β_2AR-G-protein. At the G-protein-GDP interface, the agonist has the weakest binding at -22 kcal/mol. The apo and antagonist complexes have free binding energies of -48 kcal/mol and -32 kcal/mol respectively.

The MM-GBSA binding energies (**Table 2**) clearly demonstrate destabilization through agonist binding at two interfaces of the β_2AR-G-protein complex. This is consistent with our initial results from the simulation trajectories. Agonist destabilization at both the β_2AR-G-protein and G-protein-GDP interface may likely correlate to the downstream effects of G-protein signaling. GDP leaves the agonist complex in the simulation indicating that destabilization is necessary for nucleotide exchange. The G-protein dissociates from the β_2AR after nucleotide exchange is

316 complete, indicating that destabilization at this interface is also necessary. Both the agonist (BI-
317 167107) and the antagonist (alprenolol) bind to the same binding pocket in the β_2AR. The MM-
318 GBSA values indicate the agonist binds more favorably to the β_2AR. Ligand RMSD shows
319 similar deviations within the β_2AR binding pocket and the ligands have similar key contact
320 residues (**Table 1**).

321 **Table 2: MM/GBSA (kcal/mol) Comparisons**

	No Ligand	**Antagonist**	**Agonist**
Ligand - Receptor		-125.0 ± 5.0	-185.0 ± 17.0
Receptor - G-protein	-249.0 ± 18.0	-237.0 ± 15.0	-163.0 ± 8.0
GDP - G-protein	-48.0 ± 4.0	-32.0 ± 8.0	-22.0 ± 8.0

322

323 **Conformation of GDP in the nucleotide binding pocket of Gα**

324 The conformational change of GDP in all three complexes starts at approximately the same level,
325 as shown in **Figure 4 and S14**. GDP in the agonist complex (**Figure 4A and S14A**) begins to
326 deviate significantly from the initial state and this deviation within the binding pocket indicates
327 that conformational change is necessary for GDP dissociation. Interestingly, GDP assumed
328 conformation (**Figure 5A**) similar to the co-crystallized conformation in the closed form of Gα
329 (**Figure 5B**). GDP deviation drastically changes at about 1250 ns and reaches a value of 70-75
330 Å (**Fig 4A**). The deviation stays consistent for GDP in both the apo (**Figure 4E and S14E**) and
331 antagonist bound (**Figure 4C and S14C**) complexes. MD simulation shows GDP dissociation
332 from the agonist Gα subunit only (**Figure 4A and S14A**).

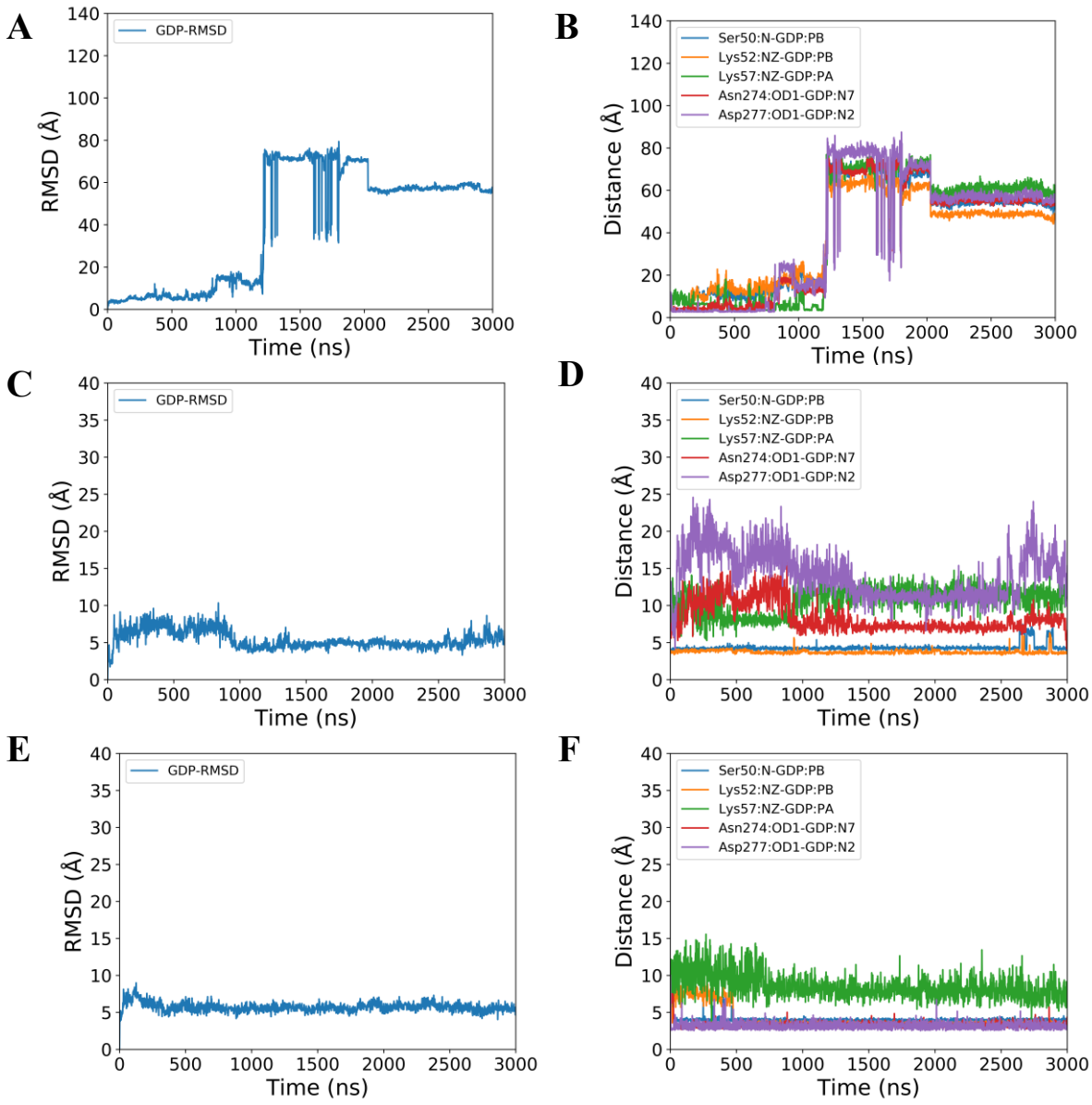

Figure 4. RMSD (left) and distances (right) between atoms of GDP and atoms of residues within binding pocket in Gαq. Agonist bound system (A and B) antagonist bound system (C and D) and apo system (E and F).

In the crystal structure (PDB ID: 1GOT) of heterotrimeric complex of Gtα-Giα chimera with Gβ and Gγ [12], GDP makes extensive interactions with P-loop and α1 helix residues. In human Gαq, $Ser50^{G.s1h1.5}$, $Gly51^{G.s1h1.6}$, $Lys52^{G.H1.1}$ and $Ser53^{G.H1.2}$ are the important residues which hold the α and β phosphates. In this crystal structure, αH domain of Gα is in contact with GDP.

For GDP release, αH domain must move away from the nucleotide binding site. Recent study by Dror et al., has revealed that GDP remains bounded to the Gα-Ras domain even after separation of αH domain [7]. In our study we also observed that GDP remains bounded to the open conformation of Gα in both antagonist (**Figure 4C and S13C**) and apo (**Figure 4E and S14E**) systems.

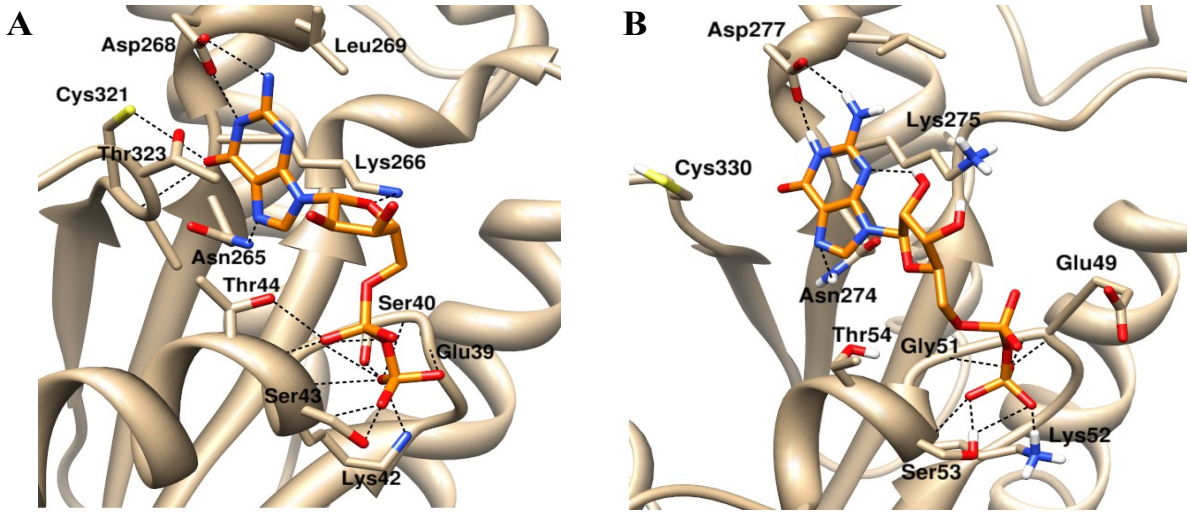

Figure 5. Conformation of GDP (orange) in (A) Crystal structure of G_t-G_i chimera (PDB ID:1GOT) and (B) Human Gαq coupled to agonist bound human β_2AR (structure extracted at t = 100 ns). H-bonds are shown in dashed black line.

In the case of agonist bound system (**Figure 4A-B and S14A-B**), GDP does not stay longer in the nucleotide binding pocket of G-alpha subunit. We observed that guanine ring of GDP rotates and makes interaction with Asn274$^{G.S5.7}$ side chain and Asp277$^{G.HG.2}$. Initially, β phosphate shows interaction with Ser50$^{G.s1h1.5}$, Gly51$^{G.s1h1.6}$, Lys52$^{G.H1.1}$ and Ser53$^{G.H1.2}$ but after 150 ns, β phosphate loses interaction with the side chain of Lys52$^{G.H1.1}$ (**Figure 4B**). Concomitant with the loss of Lys52$^{G.H1.1}$-β-phosphate interaction, another residue Lys57$^{G.H1.6}$ in the α1-helix appeared to make interaction with β phosphate. Lys57$^{G.H1.6}$ also showed interaction with α-phosphate. GDP does not show any persistent interaction with α5-β6 loop. The GDP in the agonist complex

is not in contact with any residues for at least 30.0% of the simulation time (**Table 3**). We observed similar interaction profile of GDP in the second trajectory (**Figure S14B**).

MD simulations allowed the relaxation of the GDP conformation in the nucleotide binding pocket, leading to the establishment of interactions with Asn274$^{G.S5.7}$, Lys275$^{G.s5hg.1}$ and Asp277$^{G.HG.2}$, which are also present in the template crystal structure.

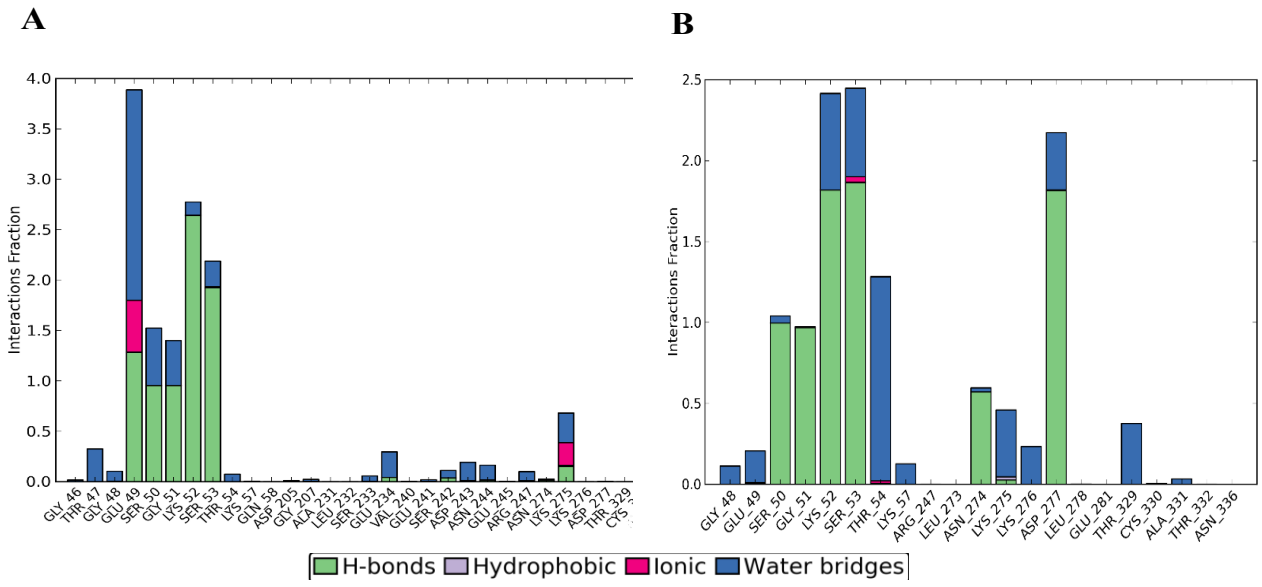

Figure 6: Histograms showing dynamic interaction profile of GDP in (A) Antagonist bound system) and (B) apo system.

In the antagonist-bound system (**Figure 4C-D and S14C-D)**, GDP showed strong interaction with P-loop residues. Only α and β phosphates interact with the residues of P-loop and α1-helix. The GDP- Gα subunit contacts are listed in **Table 3**. The 2D interaction diagrams and contact histograms for GDP in the antagonist and apo complexes are shown in **Figure 6.** Ser 50 $^{G.s1h1.5}$, Gly51$^{G.s1h1.6}$, Lys52$^{G.H1.1}$ and Ser 53$^{G.H1.2}$ are in contact with GDP in both the antagonist bound complex for at least 30.0% of the simulation time. Interaction of α and β phosphates of GDP with the side chain of Lys57$^{G.H1.6}$ was absent.

In the apo system (**Figure 4E-F and S14E-F**), guanine ring rotates while making interaction with side chain of Asp277$^{G.HG.2}$. Rotation of guanine ring leads to the establishment of H-bond between N7 and side chain of Asn274$^{G.S5.7}$. Initially, β phosphate of GDP makes strong interactions with the residues in the P-loop and α1-helix. Ser50$^{G.s1h1.5}$, Gly51$^{G.s1h1.6}$, Lys52$^{G.H1.1}$ and Ser53$^{G.H1.2}$ are the important residues which hold the β phosphate. Interactions with side chain of Asn274$^{G.S5.7}$ and Asp277$^{G.HG.2}$ persist throughout simulation. Apart from H-bonds and electrostatic interaction, GDP makes van der Waal interaction with the side chain of Lys275$^{G.S5.8}$. GDP does not show any interactions with α5-β6 loop and side chain of Lys57$^{G.H1.6}$. In the apo complex GDP is also in contact with Thr54$^{G.H1.3}$, Asn 274$^{G.S5.7}$ and Asn277$^{G.HG.2}$ for at least 30.0% of the simulation time.

Table 3. GDP-Gαq Contacts.

Agonist	Antagonist	No Ligand
S53$^{\alpha1}$*	E49$^{\alpha1}$	S50 $^{\alpha1}$
K57$^{\alpha1}$*	S50$^{\alpha1}$	G51$^{\alpha1}$
K274$^{\alpha G}$*	G51$^{\alpha1}$	K52$^{\alpha1}$
D277$^{\alpha G}$*	K52$^{\alpha1}$	S53$^{\alpha1}$
	S53$^{\alpha1}$	T54$^{\alpha1}$
		N274$^{\alpha G}$
		D277$^{\alpha G}$

*Not in contact more than 30.0% of simulation time

Trajectory images (**Figure S15**) show locations of GDP throughout the simulation for each system. GDP movement within the antagonist bound and apo systems, Gα subunits is minimal in these images. GDP movement within the agonist Gα subunit is visible. GDP appears to make conformational changes before being expelled from the Gα subunit. The GDP conformational changes within the binding pocket are indicative of coordinated communication between the activated GPCR and the G-protein. The agonist activated GPCR induces a change with the

GαRas binding pocket that induces a change in GDP binding. This is in agreement with the previous finding that opening of the Gα domains alone is not sufficient for nucleotide exchange. We also observed GDP re-attachment to the Gβ subunit which appears to be the artefact due to the limitations set by the simulation box.

Release of GDP needs strong coordinated communication between agonist bound β2-adrenergic receptor and Gα

At the β_2AR-G-protein interface, there are several regions of Gα which can receive signals from the β_2AR. However, in order to eject GDP from the nucleotide binding pocket, all signals must converge to the nucleotide binding pocket of Gα. Previous studies regarding GPCR-G-protein complex activation and nucleotide exchange provide valuable information about the nucleotide release. As stated earlier, Chung et. al. completed research to better understand the molecular workings of G-protein activation through peptide amide hydrogen-deuterium exchange mass spectrometry [6]. They determined that P-loop stabilization is a key determinant of GDP binding affinity. Dror et al., used MD simulations to analyze the Gα subunit domains and nucleotide release [7]. They determined that domain separation is necessary but not sufficient for the GDP departure. GPCR's facilitate a conformational change within the Ras domain to weaken nucleotide affinity. Dror et al., used a previous mutagenesis study to confirm this conclusion about domain separation. This mutagenesis study suggested that weakening interactions between the β6-α5 loop and GDP facilitates nucleotide release to a greater extent than increasing domain separation [32] .

Network analysis of all three systems **(Table S3-4, Figure 7 and Figure S15-23**) gave important clues about the information transfer from ligand binding site to GTP binding site. Compared to

antagonist bound system **(Figure 7B)**, communication between β_2AR and P-loop is stronger in the presence of agonist (**Figure 7A**). In case of agonist bound system, optimal path length between Asp113$^{3.32}$ of β_2AR and Ser50$^{G.s1h1.5}$ of Gα was 225. For antagonist (**Figure 7B**) and apo (**Figure 7C**) systems, optimal path lengths were 462 and 232 respectively. We observed that optimal paths of agonist bound and apo systems were similar. We found Arg60$^{G.H1.9}$ as a critical node in both 3μs and 1μs trajectories for the agonist system.

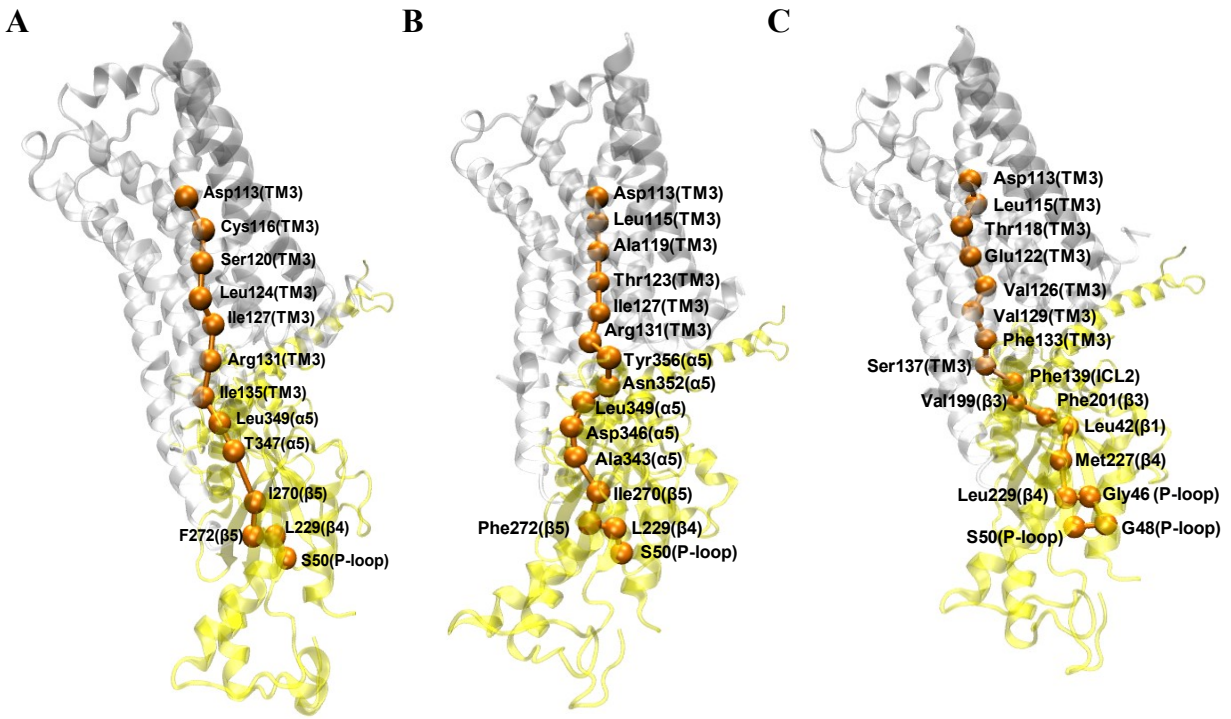

Figure 7: Optimal paths connecting the start and end points in the agonist bound system (A) antagonist bound system (B) and apo system (C). β_2AR and Gαq are shown in white and yellow color respectively.

Network analysis suggested the critical role of α5 helix in the GDP release. It is a well-established fact the α5 helix interacts with the GPCR. However, little information is available on the role of α5 helix in the GDP release. We found that signal for the GDP release starts at the Asp113$^{3.32}$ residue located on TM3 of β_2AR and reaches to P-loop via α5 helix of Gα subunit.

Optimal paths involve residues of TM3 and Gα-RAS domain. Recent study has suggested that TM3 plays very important role in the G-protein recruitment [33]. It has been reported that conformational change in α5 helix affects the nucleotide biding region by affecting β6-α5 loop and αG helix [8, 9]. Asn274$^{G.S5.7}$ and Asp277$^{G.HG.2}$ are located on β5 strand αG helix respectively. Loop connecting the αG to β5 harbours Lys275$^{G.s5hg.1}$. β5 strand forms parallel sheet with β6. In present study, residues of β6-α5 loop do not interact directly with GDP. Glu335$^{G.H5.2}$ in the α5 makes salt bridge with Arg60$^{G.H1.9}$ residue located on α1. Arg60$^{G.H1.9}$ is in close proximity to the linker (L1) region. L1 connects the Ras domain to the αH domain and it is followed by the α1 helix and P-loop. Hence any change in the α5 may affect the P-loop. Another possible way for the signal transfer is via N-terminal. Intracellular loop 2 (ICL2) of the β2 adrenergic receptor makes interaction with the residues of αN and αN-β1 loop. However, in optimal paths we did not see any residue belonging to αN and αN-β1 loop. In the network analysis, we observed that residues in the β4 (L229$^{G.S4.5}$) and β5 (I270$^{G.S5.3}$ and F272$^{G.S5.5}$) strands are part of the optimal path between agonist binding site and GDP binding site. Both I270$^{G.S5.3}$ and F272$^{G.S5.5}$ are conserved across different families of Gα (Figure S1). Recent study suggests the role of β1-β3 strands in GDP release [9] but role of β4-β5 has not been reported.

We also analyzed the important interactions at β_2AR-Gα interface (**Figure 8**). C-terminal region of α5-helix of Gα interacts with the transmembrane region of the β_2-AR. We observed interaction between Arg131$^{3.50}$ of β2-AR and Tyr356$^{G.H5.23}$ of Gα at side chain level. Distance between center of mass of Arg131$^{3.50}$ and Tyr356$^{G.H5.23}$ was calculated for all three systems. In agonist bound system (**Figure 8A and B**), compared to the antagonist bound system (**Figure 8C and D**) and apo system (**Figure 8E and F**), average distance was relatively smaller (8.16Å for agonist, 9.43 Å for antagonist and 9.92 Å for no ligand) and more stable till 2μs. In the 1μs

trajectory (**Figure S24**), we observed a similar trend (8.44Å for agonist, 8.87 Å for antagonist and 9.34 Å for no ligand). It is clear that in the agonist bound system α5 helix of Gα interacts strongly with TM3 of β_2-AR. Previous study[5] has reported about the interaction between Arg131$^{3.50}$ and Tyr356$^{G.H5.23}$ but its role in the GDP release has not been discussed. In a study by Goetz et al., 2011[34] , compared to inverse agonist and antagonist, agonist bound β_2AR complex exhibited stable binding with G_αCT. In other study [35], crystal structure of agonist bound β_2AR with GαCT showed that GαCT assumed different conformation in which R389 and E392 of Gαs exhibited interactions with Asp130$^{3.49}$ and Arg131$^{3.50}$ of β_2AR. Authors have hypothesized that above interactions may initiate GDP release. In $G_{\alpha q}$, R389$^{G\alpha s}$ and E392$^{G\alpha s}$ are replaced by K354$^{G\alpha q}$ and N357$^{G\alpha q}$ respectively. In our study we observed that G_αCT maintained the similar conformation as reported in the crystal structure of β_2AR-G protein and Y356 of Gαq exhibited interaction with Arg131. It is possible that the association of G-protein with activated β_2AR may involve several intermediate steps.

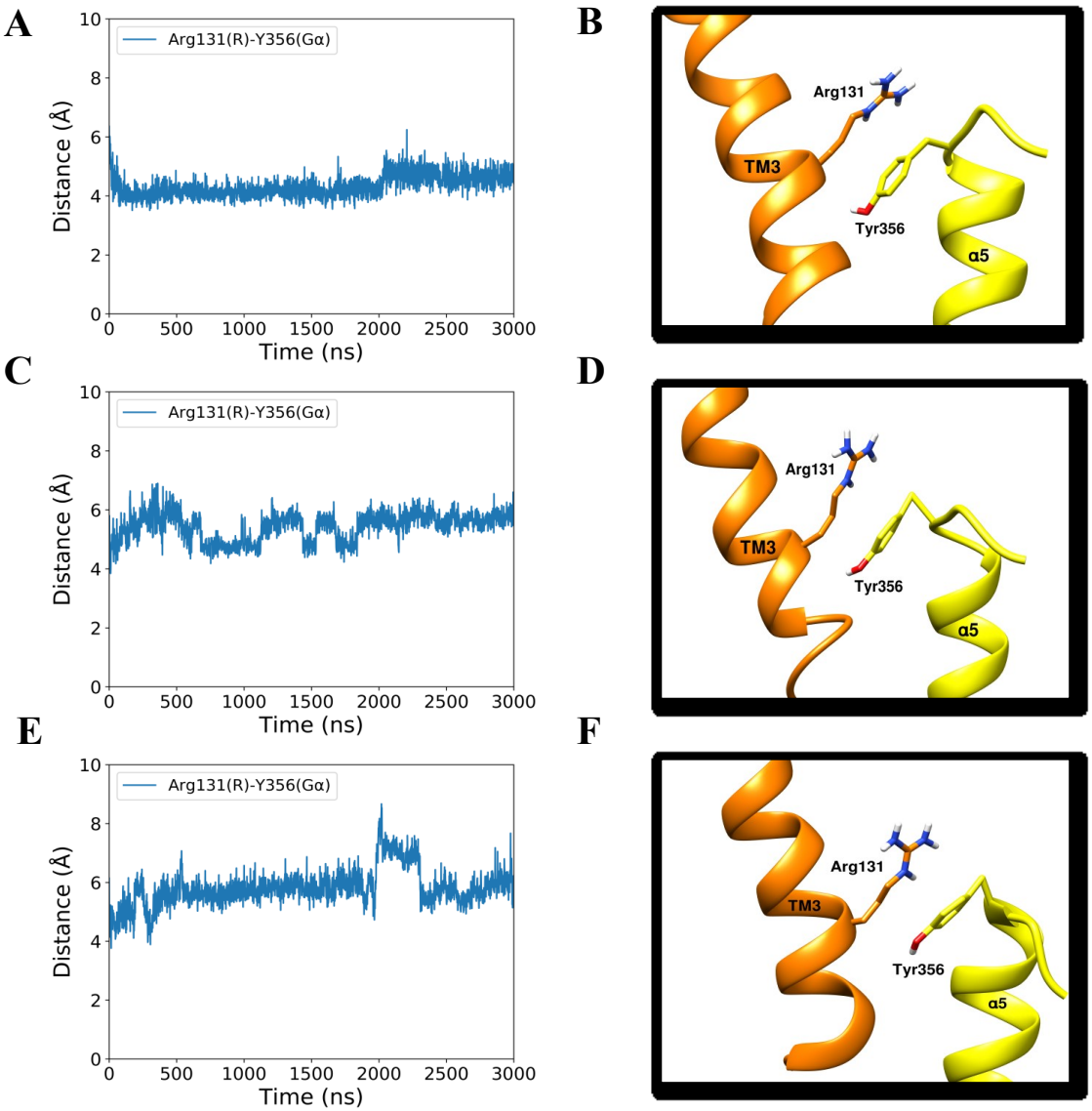

464

465 **Figure 8**. Distances between center of mass of Arg131$^{3.50}$ (β_2AR) and Tyr356$^{G.H5.23}$ (Gαq) in
466 agonist bound system (A) antagonist bound system (C) and apo system (E). Snapshot taken at
467 1μs showing interaction between Arg131$^{3.50}$ and Tyr356$^{G.H5.23}$ in agonist bound system (B)
468 antagonist bound system (D) and apo system (F).

469

470 **Effect of agonist and antagonist on interdomain distance in the open conformation of Gα**

As discussed previously, separation of αH domain and Ras domain is important for the GDP release. In the crystal structure of β_2AR-$G_{\alpha s}$-protein (PDB ID:3SN6), interdomain distance is 62.68Å (distance between Cα atoms of Ala161$^{H.HE.6}$ and Glu299$^{G.hgh4.9}$). We observed that interdomain distance does not change significantly when Gαq is coupled to either agonist or antagonist bound β_2AR. In the apo system, average interdomain distance was 65.13Å (**Table 4**). In the presence of agonist and antagonist, average interdomain distances were 61.75Å and 67.43Å respectively (**Table 4**). We see that average interdomain distance in the agonist bound system stays very close to the distance observed in the crystal structure. However, we think that longer simulation time is required to see the effect of ligands on interdomain distance between αH and RAS domains.

Table 4. **Average interdomain distance between αH and Ras domains. Distance was calculated between Cα atoms of Glu143$^{H.HE.6}$ and Glu281$^{G.hgh4.9}$.**

System	Average interdomain distance (Å)
Agonist	61.75 ± 2.00
Antagonist	67.47 ± 1.98
Apo	65.13 ± 1.51

Residues in the α1 helix of the Gα control the release of GDP

It is important to discuss the relative contributions of different types of interactions which keep the GDP in the pocket. Residues in the nucleotide binding pocket which interact with either α or β phosphate or both have greater impact on the GDP conformation and position. In the agonist system, we observed that interaction of β-phosphate of GDP with the side chain of Lys52$^{G.H1.1}$

disappears before 200 ns and this loss of interaction leads to the establishment of salt bridge between Lys52$^{G.H1.1}$ and Asp205$^{G.S3.7}$ (**Figure 9A**), also observed in the second trajectory of agonist system **(Figure S25A**).

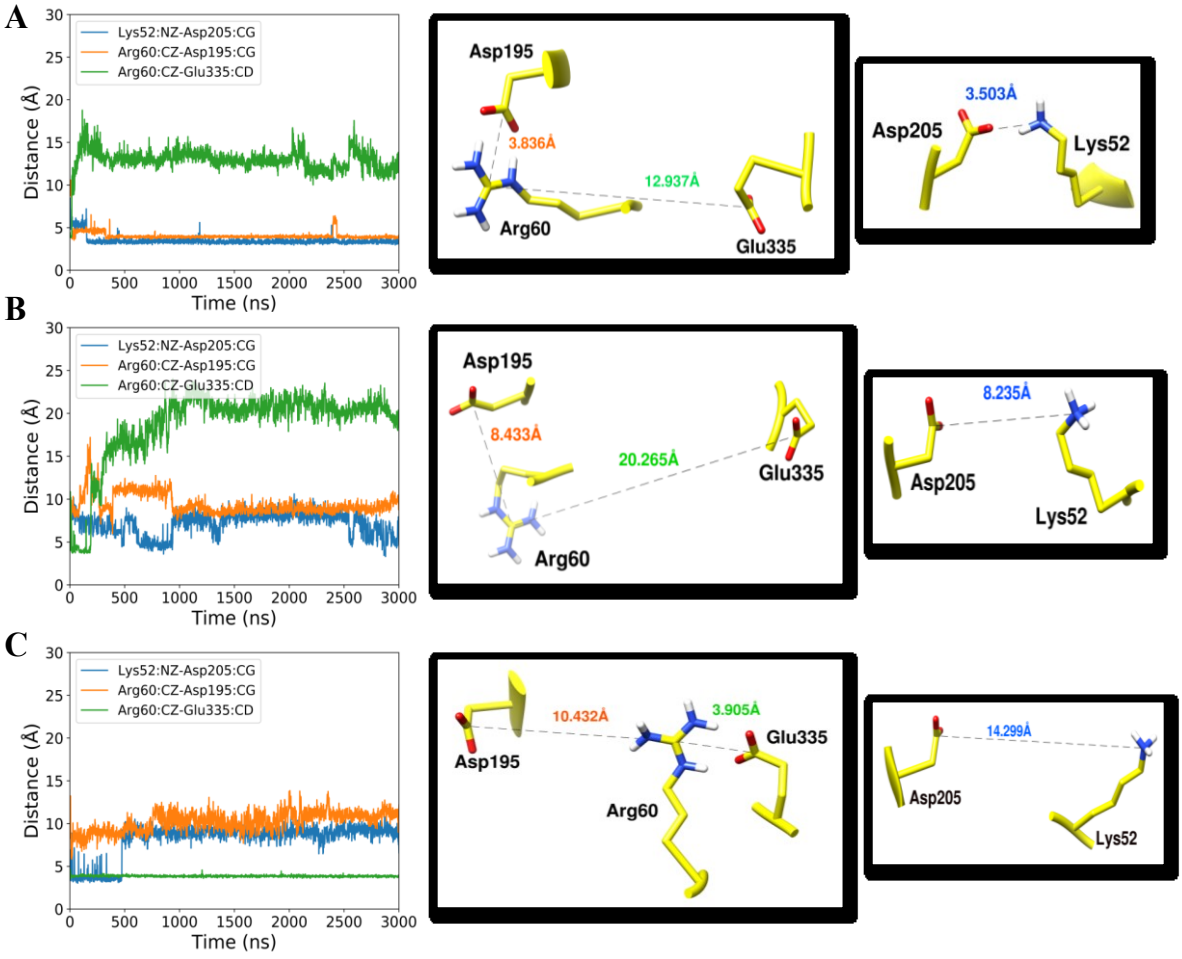

Figure 9. Breakage and formation of salt bridges near nucleotide binding pocket in the Gαq. (A) Agonist bound system (B) antagonist bound system and (C) apo system. All residues belong to Gαq.

After losing the interaction with Lys52$^{G.H1.1}$ side chain, Lys57$^{G.H1.6}$ sidechain initialized the interaction with the α phosphate, subsequently led to the movement of α phosphate group towards the side chain of Lys57$^{G.H1.6}$. Interaction of GDP with Lys57$^{G.H1.6}$ was only present in

the agonist bound system. 1 μs trajectory of agonist bound system (**Figure S9B**) also substantiated the role of Lys57$^{G.H1.1}$ in GDP release. Lys52$^{G.H1.1}$-Asp205$^{G.S3.7}$ salt bridge was not present in two trajectories of antagonist system **(Figure 9B** and **S25B**) and one trajectory of apo system (**Figure 9C**). However, in the other trajectory of apo system (**Figure S25C**), Lys52$^{G.H1.1}$-Asp205$^{G.S3.7}$ salt bridge was present and interactions of β-phosphate with Lys52$^{G.H1.1}$ and residues of P-loop were absent. According to Chung et al.,[6] P-loop stabilization and β-phosphate coordination are important for GDP(and GTP) affinity. In a computational study by Louet et al.,[39] it was found that in heterotrimeric G-proteins, GDP release preferentially occurs on the phosphate side. Another important interaction which may play key role in the GDP release is the breakage and formation of salt bridges involving Arg60$^{G.H1.9}$. We observed that Arg60$^{G.H1.9}$-Asp195$^{G.S2.7}$ salt bridge is only present in the Gαq of agonist bound system (**Figure 9A and S25A**). Recent study by Sun et al., suggests the role of α1 helix in GDP release [9]. Mutational studies have shown that mutations of Lys52$^{G.H1.1}$, Lys57$^{G.H1.6}$ and Arg60$^{G.H1.9}$ affect the stability of Gα-GDP complex [31]. Arg60$^{G.H1.9}$Cys mutation has been reported to cause autosomal dominant hypo-parathyroidism by affecting the H-domain opening and GDP release [31]. We found that Arg60$^{G.H1.9}$ acts as a critical node in the network map of agonist bound system (**Table S3 and S4**).

Summary of the agonist induced GDP release from the open conformation of Gα. Before release of first crystal structure of agonist bound GPCR-Gαβγ complex (PDB ID: 3SN6), different models were proposed to explain the GDP release [8]. One of the models known as "lever-arm" suggests that $G_{\beta\gamma}$ complex acts as lever which tilts the $G_{\alpha,}$ leading to opening of the nucleotide binding pocket [36, 37] . Other model known as "gear-shift" suggests that GPCR uses N-terminus of G_{α} to shift the $G_{\beta\gamma}$ towards the G_{α} [38]. Shifting of $G_{\beta\gamma}$ towards G_{α} induces

conformational change in α5 helix. Above models became less significant after the release of crystal structure of agonist bound GPCR-Gαβγ complex which shows engagement of α5 helix with the GPCR. Crystal structure shows that GPCR bound Gα is in open conformation. Previous "α5-centered" models have not addressed the GDP release from the open conformation of Gα in the presence of agonist bound β_2AR, considering only β_2AR free nucleotide bound G_α [9] or nucleotide free β_2AR-G_α [7]. Therefore we carried out multiple microseconds MD simulations to provide a structural view of allosteric communication between agonist binding pocket of β_2AR and nucleotide bound to the open conformation of G_α. MD simulations revealed that binding of agonist is necessary for the GDP release for the first time. In two independent simulations, GDP moves out of the nucleotide binding pocket. Interestingly, in both trajectories, GDP leaves the nucleotide binding pocket in similar fashion. We observed that exit route of GDP involves α1 and α5 helices. It is noteworthy that in both agonist bound and apo systems, GDP undergoes conformational change in similar fashion. Based on the MD simulation results, we have summarized the information transfer from agonist binding site to GDP in the pictorial form (**Figure 10 and 11**). Figure 10, shows that the GDP release is an outcome of coordination of multiple residues belonging to different regions of β_2AR and Gα. From the β_2AR side, we found that TM3 helix plays critical role in the signal transfer to the open conformation of Gα subunit. We found that the interaction between $Arg131^{3.50}$ of DRY motif and $Y356^{G.H5.23}$ of α5, acts as a bridge to link the information flow from receptor to the G_α In particular, in the presence of agonist, $Arg131^{3.50}$ of DRY motif forms strong cation-π interaction with $Y356^{G.H5.23}$ of α5. In $G_{\alpha i}$, mutation of residue at equivalent position (G.H5.23) affect the stability of GPCR-$G_{\alpha i}$ complex[31]. Mutations in the C-terminal of α_t have been reported to affect the G-protein activation [40]. Recent computational study has also shown that displacement of α5 helix induces GDP release [9]. Our

findings strongly support the dominant role of α5 helix in the release of GDP from the open conformation of G_α. Furthermore, our communication network model appears to provide more complete picture than the early models including the "α5-centered models". Encouragingly, key residues and secondary elements identified in our communication network are consistent with the experimental studies. We observed that agonist induced perturbations in the β_2AR travel to Gα and eventually abolish the electrostatic interactions of α and β phosphates of GDP within the nucleotide binding pocket (**Figure 4**). Overall our study suggests that agonist binding to the β_2AR is prerequisite for the GDP release (**Figure 10 and 11**).

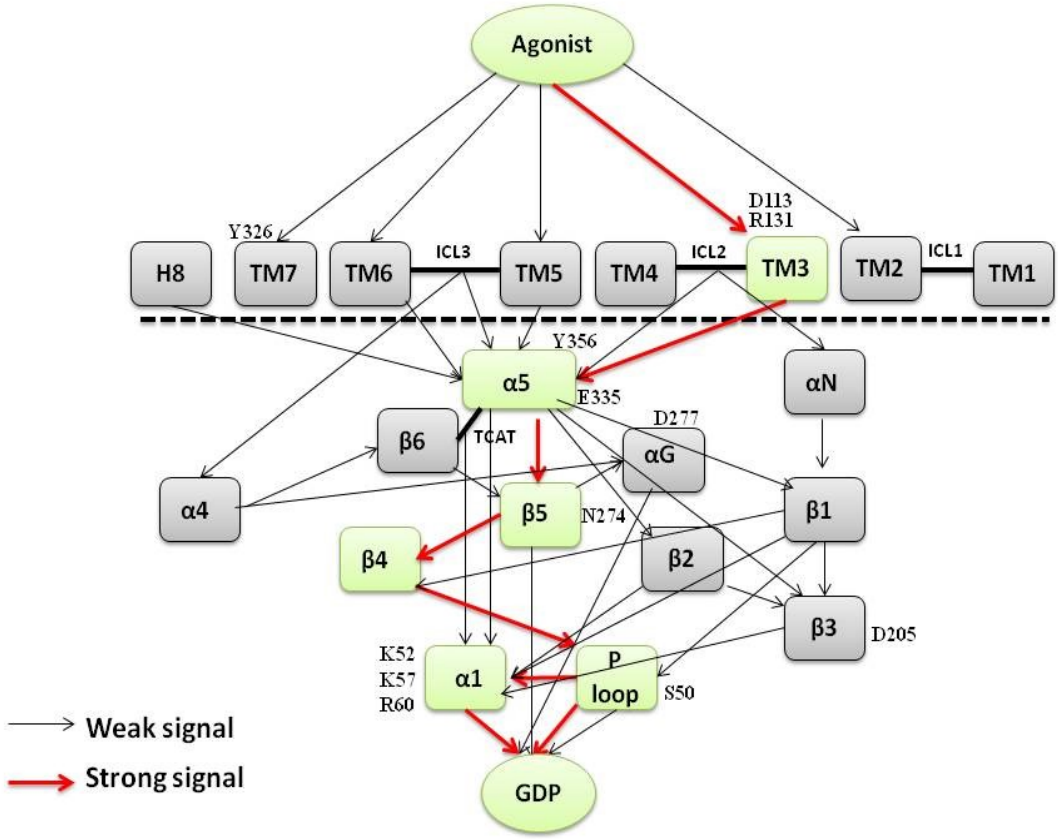

Figure 10. Strong communication pathway involves red solid arrows and light green boxes. Important residues involved in the allosteric communication have been highlighted.

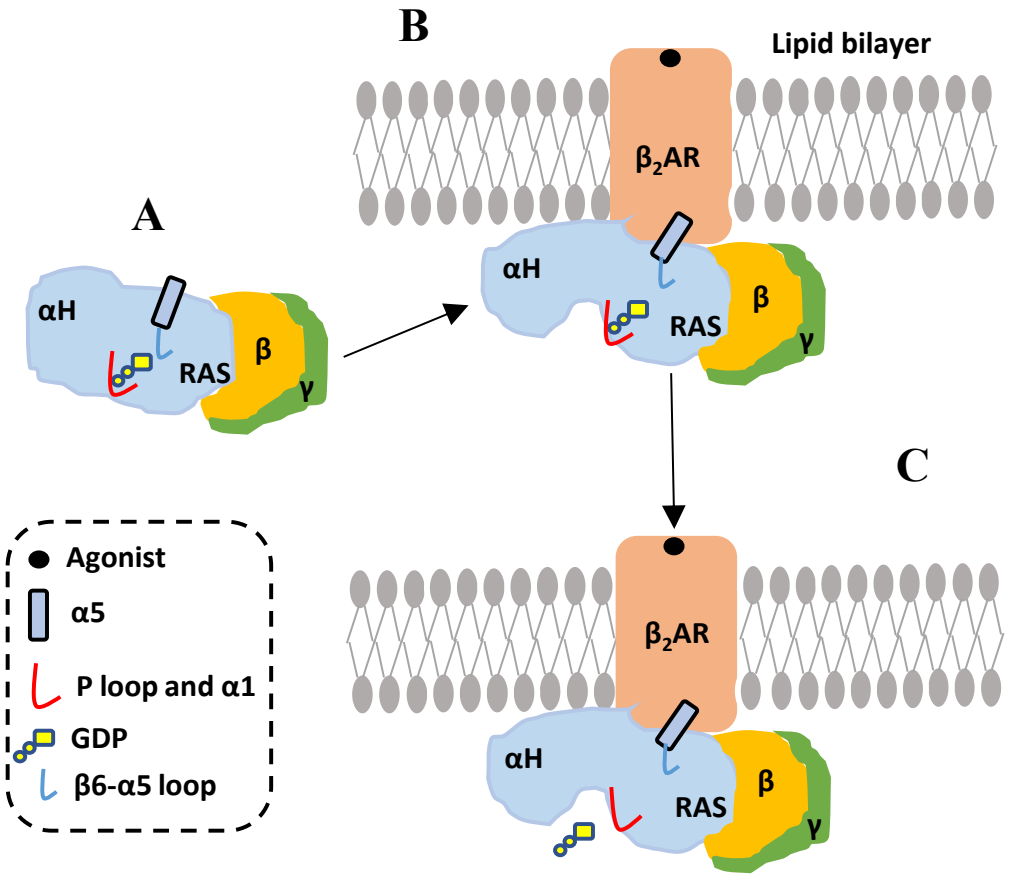

Figure 11. GDP release mechanism. (A) GDP tightly bound to closed conformation of G_{α} in the receptor free $G_{\alpha\beta\gamma}$ complex (PDB 1GOT) (B) GDP bound Gαβγ complex interacts with activated receptor and α5 docks into the intracellular cavity of β_2AR. α5 is pulled towards the receptor and subsequently β6-α5 loop moves away from the guanine ring of GDP. Open conformation of Gα gets stabilized. Movement of αH domain also affects P-loop and α1. (C) Allosteric signal passes through α5 and propagates to the P loop and α1 and conformational change in P loop and α1 leads to the release of GDP (PDB 3SN6).

Conclusions

MD simulations demonstrate the effects of an agonist and an antagonist on G-protein activation and therefore nucleotide exchange. MM-GBSA analysis shows the destabilization of the GPCR-G-protein complex due to agonist binding. The binding of antagonist has a smaller destabilization effect. This destabilization is likely to be the preparation for GDP release and G-protein dissociation. While the tyrosine toggle switch (NPXXY) appears to be activated in the agonist complex, we argue that molecular switches might not crucial for this β_2AR-G-protein activation. The RMSD and RMSF analyses revealed important conformational changes within the GPCR and G-protein. The largest changes within the receptor occur at the ECL2 and ICL3. The Gα subunit plays the largest role in G-protein activation and GDP release. Residue interaction network analysis revealed the coordinated communication paths between agonist/antagonist binding pocket and GDP binding pocket. We found that α5 helix receives the signal from the agonist bound β_2AR and transmit to the other parts of Gα. In the agonist bound system, strong interaction between TM3 and C-terminus of α5 helix promotes the GDP release. Conserved residues of α1-helix responsible for the release of GDP were also identified for the experimental validation. Present study will be helpful in understanding the mechanism of Gα activation and nucleotide exchange.

Acknowledgements

C.W acknowledges the support by Rowan SEED grant and the National Science Foundation under Grants NSF ACI-1429467/RUI-1904797, and XSEDE MCB 170088. The Anton2 machine at the Pittsburgh Supercomputing Center (PSCA17017P) was generously made available by D. E. Shaw Research. The grants from National Natural Science Foundation of China (11575021, U1530402) to H.L. are also acknowledged.

Supporting information available:

Supporting information contains 4 tables (Table S1 to S4) and 25 figures (Figure S1 to S25).

References:

1. Zhang, D.; Zhao, Q.; Wu, B., Structural Studies of G Protein-Coupled Receptors. *Mol. Cells* **2015**, *38*, 836-42.
2. Hauser, A. S.; Attwood, M. M.; Rask-Andersen, M.; Schioth, H. B.; Gloriam, D. E., Trends in GPCR drug discovery: new agents, targets and indications. *Nat. Rev. Drug Discov.* **2017**, *16*, 829-842.
3. Hilger, D.; Masureel, M.; Kobilka, B. K., Structure and dynamics of GPCR signaling complexes. *Nat. Struct. Mol. Biol.* **2018**, *25*, 4-12.
4. Jastrzebska, B., GPCR: G protein complexes--the fundamental signaling assembly. *Amino Acids* **2013**, *45*, 1303-14.
5. Rasmussen, S. G. F.; DeVree, B. T.; Zou, Y. Z.; Kruse, A. C.; Chung, K. Y.; Kobilka, T. S.; Thian, F. S.; Chae, P. S.; Pardon, E.; Calinski, D.; Mathiesen, J. M.; Shah, S. T. A.; Lyons, J. A.; Caffrey, M.; Gellman, S. H.; Steyaert, J.; Skiniotis, G.; Weis, W. I.; Sunahara, R. K.; Kobilka, B. K., Crystal structure of the beta(2) adrenergic receptor-Gs protein complex. *Nature* **2011**, *477*, 549-U311.
6. Chung, K. Y.; Rasmussen, S. G.; Liu, T.; Li, S.; DeVree, B. T.; Chae, P. S.; Calinski, D.; Kobilka, B. K.; Woods, V. L., Jr.; Sunahara, R. K., Conformational changes in the G protein Gs induced by the beta2 adrenergic receptor. *Nature* **2011**, *477*, 611-5.
7. Dror, R. O.; Mildorf, T. J.; Hilger, D.; Manglik, A.; Borhani, D. W.; Arlow, D. H.; Philippsen, A.; Villanueva, N.; Yang, Z. Y.; Lerch, M. T.; Hubbell, W. L.; Kobilka, B. K.; Sunahara, R. K.; Shaw, D. E., Structural basis for nucleotide exchange in heterotrimeric G proteins. *Science* **2015**, *348*, 1361-1365.
8. Raimondi, F.; Seeber, M.; De Benedetti, P. G.; Fanelli, F., Mechanisms of inter- and intramolecular communication in GPCRs and G proteins. *J. Am. Chem. Soc.* **2008**, *130*, 4310-4325.
9. Sun, X.; Singh, S.; Blumer, K. J.; Bowman, G. R., Simulation of spontaneous G protein activation reveals a new intermediate driving GDP unbinding. *Elife* **2018**, *7*.
10. Lomize, M. A.; Pogozheva, I. D.; Joo, H.; Mosberg, H. I.; Lomize, A. L., OPM database and PPM web server: resources for positioning of proteins in membranes. *Nucleic Acids Res.* **2011**, *40*, D370-D376.
11. Wacker, D.; Fenalti, G.; Brown, M. A.; Katritch, V.; Abagyan, R.; Cherezov, V.; Stevens, R. C., Conserved Binding Mode of Human β2 Adrenergic Receptor Inverse Agonists and Antagonist Revealed by X-ray Crystallography. *J. Am. Chem. Soc.* **2010**, *132*, 11443-11445.
12. Lambright, D. G.; Sondek, J.; Bohm, A.; Skiba, N. P.; Hamm, H. E.; Sigler, P. B., The 2.0 Å crystal structure of a heterotrimeric G protein. *Nature* **1996**, *379*, 311-319.

13. Jambeck, J. P.; Lyubartsev, A. P., An Extension and Further Validation of an All-Atomistic Force Field for Biological Membranes. *J Chem Theory Comput* **2012**, *8*, 2938-48.
14. Pan, D. S.; Wang, W.; Liu, N. S.; Yang, Q. J.; Zhang, K.; Zhu, J. Z.; Shan, S.; Li, Z. B.; Ning, Z. Q.; Huang, L. Q.; Lu, X. P., Chiglitazar Preferentially Regulates Gene Expression via Configuration-Restricted Binding and Phosphorylation Inhibition of PPAR gamma. *Ppar Research* **2017**.
15. Ebadi, A.; Dastan, D.; Azami, M.; Karimi, A.; Razzaghi-Asl, N., Molecular Modeling of Human CCR2 Receptor within POPC Lipid Bilayer. *Structural Chemistry* **2016**, *28*, 849-857.
16. Khatami, M. H.; Saika-Voivod, I.; Booth, V., All-atom molecular dynamics simulations of lung surfactant protein B: Structural features of SP-B promote lipid reorganization. *Biochim. Biophys. Acta, Biomembr.* **2016**, *1858*, 3082-3092.
17. Khatami, M. H.; Bromberek, M.; Saika-Voivod, I.; Booth, V., Molecular dynamics simulations of histidine-containing cod antimicrobial peptide paralogs in self-assembled bilayers. *Biochim. Biophys. Acta, Biomembr.* **2014**, *1838*, 2778-2787.
18. Mark, P.; Nilsson, L., Structure and Dynamics of the TIP3P, SPC, and SPC/E Water Models at 298 K. *J. Phys. Chem. A* **2001**, *105*, 9954-9960.
19. Harder, E.; Damm, W.; Maple, J.; Wu, C.; Reboul, M.; Xiang, J. Y.; Wang, L.; Lupyan, D.; Dahlgren, M. K.; Knight, J. L.; Kaus, J. W.; Cerutti, D. S.; Krilov, G.; Jorgensen, W. L.; Abel, R.; Friesner, R. A., OPLS3: A Force Field Providing Broad Coverage of Drug-like Small Molecules and Proteins. *J. Chem. Theory Comput.* **2016**.
20. Humphrey, W.; Dalke, A.; Schulten, K., VMD: Visual molecular dynamics. *J. Mol. Graphics* **1996**, *14*, 33-38.
21. Sethi, A.; Eargle, J.; Black, A. A.; Luthey-Schulten, Z., Dynamical networks in tRNA:protein complexes. *Proc. Natl. Acad. Sci.* **2009**, *106*, 6620.
22. Glykos, N. M., Software news and updates carma: A molecular dynamics analysis program. *J. Comput. Chem.* **2006**, *27*, 1765-1768.
23. Eargle, J.; Luthey-Schulten, Z., NetworkView: 3D display and analysis of protein·RNA interaction networks. *Bioinformatics* **2012**, *28*, 3000-3001.
24. Bhattacharyya, M.; Bhat, C. R.; Vishveshwara, S., An Automated Approach to Network Features of Protein Structure Ensembles. *Protein Sci.* **2013**, *22*, 1399-1416.
25. Gadiyaram, V.; Vishveshwara, S.; Vishveshwara, S., From Quantum Chemistry to Networks in Biology: A Graph Spectral Approach to Protein Structure Analyses. *J. Chem. Inf. Model.* **2019**, *59*, 1715-1727.
26. Stolzenberg, S.; Michino, M.; LeVine, M. V.; Weinstein, H.; Shi, L., Computational Approaches to Detect Allosteric Pathways in Transmembrane Molecular Machines. *Biochim. Biophys. Acta, Biomembr.* **2016**, *1858*, 1652-1662.
27. Schneider, S.; Provasi, D.; Filizola, M., How Oliceridine (TRV-130) Binds and Stabilizes a μ-Opioid Receptor Conformational State That Selectively Triggers G Protein Signaling Pathways. *Biochemistry* **2016**, *55*, 6456-6466.
28. Jiang, Y.; Yuan, Y.; Zhang, X.; Liang, T.; Guo, Y.; Li, M.; Pu, X., Use of Network Model to Explore Dynamic and Allosteric Properties of Three GPCR Homodimers. *RSC Adv.* **2016**, *6*, 106327-106339.
29. Genheden, S.; Ryde, U., The MM/PBSA and MM/GBSA methods to estimate ligand-binding affinities. *Expert Opin. Drug Discovery* **2015**, *10*, 449-461.
30. Li, J.; Abel, R.; Zhu, K.; Cao, Y.; Zhao, S.; Friesner, R. A., The VSGB 2.0 model: A next generation energy model for high resolution protein structure modeling. *Proteins: Struct., Funct., Bioinf.* **2011**, *79*, 2794-2812.
31. Flock, T.; Ravarani, C. N. J.; Sun, D.; Venkatakrishnan, A. J.; Kayikci, M.; Tate, C. G.; Veprintsev, D. B.; Babu, M. M., Universal allosteric mechanism for Gα activation by GPCRs. *Nature* **2015**, *524*, 173-179.
32. Marin, E. P.; Krishna, A. G.; Archambault, V.; Simuni, E.; Fu, W.-Y.; Sakmar, T. P., The Function of Interdomain Interactions in Controlling Nucleotide Exchange Rates in Transducin. *J. Biol. Chem.* **2001**, *276*, 23873-23880.
33. Zhou, Q.; Yang, D.; Wu, M.; Guo, Y.; Guo, W.; Zhong, L.; Cai, X.; Dai, A.; Jang, W.; Shakhnovich, E. I.; Liu, Z.-J.; Stevens, R. C.; Lambert, N. A.; Babu, M. M.; Wang, M.-W.; Zhao, S., Common activation mechanism of class A GPCRs. *eLife* **2019**, *8*, e50279.
34. Goetz, A.; Lanig, H.; Gmeiner, P.; Clark, T., Molecular Dynamics Simulations of the Effect of the G-Protein and Diffusible Ligands on the β2-Adrenergic Receptor. *J. Mol. Biol.* **2011**, *414*, 611-623.
35. Liu, X.; Xu, X.; Hilger, D.; Aschauer, P.; Tiemann, J. K. S.; Du, Y.; Liu, H.; Hirata, K.; Sun, X.; Guixà-González, R.; Mathiesen, J. M.; Hildebrand, P. W.; Kobilka, B. K., Structural Insights into the Process of GPCR-G Protein Complex Formation. *Cell* **2019**, *177*, 1243-1251.e12.

36. Iiri, T.; Farfel, Z.; Bourne, H. R., G-protein diseases furnish a model for the turn-on switch. *Nature* **1998**, *394*, 35-38.
37. Rondard, P.; Iiri, T.; Srinivasan, S.; Meng, E.; Fujita, T.; Bourne, H. R., Mutant G protein α subunit activated by Gβγ: A model for receptor activation? *Proc. Natl. Acad. Sci.* **2001**, *98*, 6150-6155.
38. Cherfils, J.; Chabre, M., Activation of G-protein Gα subunits by receptors through Gα-Gβ and Gα-Gγ interactions. *Trends Biochem. Sci.* **2003**, *28*, 13-17.
39. Louet, M.; Martinez, J.; Floquet, N., GDP Release Preferentially Occurs on the Phosphate Side in Heterotrimeric G-proteins. *PLoS Comput. Biol.* **2012**, *8*, e1002595.
40. Natochin, M.; Moussaif, M.; Artemyev, N. O., Probing the mechanism of rhodopsin-catalyzed transducin activation. *J. Neurochem.* **2001**, *77*, 202-210.

Table of Contents graphics